RADIATIVE FORCING OF SAHARAN AEROSOLS IN THE VISIBLE REGION

*B. I. Tijjani and **R. S. Sa'id
Department of Physics, Bayero University, Kano.
Emails: *idrith@yahoo.com, idrithtijjani@gmail.com,**rabisalihu@gmail.com.

ABSTRACT

We study the aerosol radiative forcing (RF) at visible wavelengths (0.40 μm to 0.75μm) and relative humidity (RH) 0, 50, 70, 80, 90, 95, 98, and 99% using data from the Optical Properties of Aerosol and Clouds software. The primary influence on direct radiative forcing by aerosols are its wavelength dependence scattering, absorption and extinction coefficients, asymmetric parameter, single scattering albedo and other optical parameters which also depend strongly on relative humidity (RH). The dependence of optical depth on wavelengths is quantified in terms of Angstrom exponent, which provides information on the sizes of particles that are dominant in contributing to the optical depths and the RFs. In terms of these parameters, Saharan aerosols were analysed in this paper and several findings were determined. One of the finding showed that the Angstrom exponent increases from 0.0466 to 0.3395 as a result of hygroscopic growth and also that, increase in RH has caused mode size growth. The analysis further shows that these aerosols have Junge type of size distributions and are dominated by coarse mode particles distribution.

INTRODUCTION

Aerosol particles contribute a lot in global and regional climate change by backscattering and absorbtion of solar radiation [1,2]. It has been speculated that aerosol particles could contribute to global and regional dimming [3,4] and a change in regional precipitation [5]. Dust aerosols from the original source regions can be transported thousands of kilometers away [6-9].

Among all the different types of atmospheric aerosols, desert dust is of primary importance, first of all, because the extension of its potential source areas covers about one-third of the terrestrial surface; a further aspect which renders the desert aerosol one of the most prominent aerosol types is the long-range atmospheric transport due to strong winds and convective processes [10].

To better understand the radiative forcing, analysis of aerosol optical properties and their dependency on relative humidity (RH) is needed [11-13]. Hygroscopicity is one of the most important fundamental properties of atmospheric aerosols. By absorbing water, atmospheric hygroscopic aerosols change their sizes and chemical compositions, thereby affecting their deposition characteristics, size distributions, radiative properties, and chemical reactivity. The change in for example light-scattering (or extinction, optical depth, absorption, single scattering albedo, asymmetric parameters) by aerosols with RH at a specific wavelength, f(RH, λ), (hygroscopic growth factor or humidification factor), has been considered an important parameter to estimate and describe the nature of aerosol Radiative forcing [2,12,14-19] and to understand the cause of visibility degradation due to aerosols [20-22] showed from laboratory and aircraft campaign that dust particles can initiate ice formation at relatively warm and dry conditions in the atmosphere. This effect has been observed in Saharan dust plumes.

In this paper the data about the optical and microphysical properties for the Saharan dust at visible region (0.4 to 0.75μm) are extracted from OPAC. Radiative forcing at different wavelength and Relative humidity are calculated and plotted. To better understand and be able to analysed the nature and the type of interaction of particles in the Saharan aerosols, the effective refractive indices, optical depths, single scattering albedo, asymmetric parameters and extinction scattering and absorption coefficients are analysed with respect to wavelength and relative humidities.

METHODOLOGY

The data used for the Saharan aerosols are derived from the Optical Properties of Aerosols and Clouds (OPAC) data set [23]. In this, a mixture of four components is used to describe desert aerosols: a water soluble components (WASO), and three mineral components of different sizes – mineral nucleation mode (MINM), mineral accumulation mode (MIAM) and mineral coarse mode (MICM).

The globally averaged direct aerosol Radiative forcing, ΔF_R, for absorbing aerosols was calculated using the equation derived by [24]

$$\Delta F_R = -\frac{S_0}{4} T_{atm}^2 (1-N)\{(1-A)^2 2\beta\tau_{sca} - 4A\tau_{abs}\} \quad (1)$$

Where S_0 is a solar constant, T_{atm} is the transmittance of the atmosphere above the aerosol layer, N is the fraction of the sky covered by clouds, A is the albedo of underlying surface, β is the upscattering fraction of radiation scattered by aerosol into the atmosphere while τ_{sca} and τ_{abs} are the aerosol layer scattering and absorptions optical thickness respectively [25]. The above expression gives the radiative forcing due to the change of reflectance of the earth-aerosol system. The upscattering fraction is calculated using an approximate relation [26]

$$\beta = \frac{(1-g/2)}{2} \quad (2)$$

The global averaged albedo A=0.22 over land and A=0.06 over the ocean with 80% of aerosols being over the land; solar constant of 1370Wm^{-2}, the atmospheric transmittance is taken to be T_{atm}=0.79 [25] and cloudness N=0.6.

To determine the effective refractive indices the following formula is used for the four mixed aerosols [27]:

$$\frac{\varepsilon_{eff}-\varepsilon_0}{\varepsilon_{eff}+2\varepsilon_0} = \sum_{i=1}^{4} f_i \frac{\varepsilon_i-\varepsilon_0}{\varepsilon_i+2\varepsilon_0} \quad (3)$$

Where f_i and ε_i are the volume fraction and dielectric constant of the i^{th} component and ε_0 is the dielectric constant of the host material. For the case of Lorentz-Lorentz [28,29], the host material is taken to be vacuum, $\varepsilon_0 = 1$.

The spectral behavior of the aerosol optical thickness, scattering, absorption, and extinction coefficients can be used to obtain some information regarding the size distribution by just looking at the Angstron coefficient exponent that expresses the spectral dependence of aerosol optical depth (τ), scattering (σ_{scat}), absorption (σ_{abs}) and extinction (σ_{ext}) coefficients, with the wavelength of light (λ) as inverse power law:

$$X(\lambda)=\beta\lambda^{-\alpha} \quad (4)$$

Where the wavelength dependence $X(\lambda)$ (can be aerosol optical depth (τ), scattering (σ_{scat}), absorption (σ_{abs}) and extinction (σ_{ext}) coefficients). But since τ is the simplest and more significant magnitude to characterize the columnar atmospheric aerosol load [30], $X(\lambda)$ is replaced by $\tau(\lambda)$, which can be characterized by the Angstron parameter, which is a coefficient of the following regression:

$$\ln \tau(\lambda) = -\alpha \ln(\lambda) + \ln\beta \quad (5)$$

where β and α are the turbidity coefficient and the shaping factor, respectively [31,32]. The turbidity coefficient is a proportionality constant relating the optical depth and the wavelength. The shaping factor α provides a measure of how rapidly aerosol optical depth τ changes with wavelength and also relates to the size of particles. The value of α depends on the ratio of the concentration of large to small aerosols and β represents the total aerosol loading in the atmosphere. So α and β can also be used to describe the size distribution of aerosol particles and

the general haziness of the atmosphere. Larger particles generally correspond to smaller α, whereas smaller particles generally correspond to larger α. According to [33] a low (down to 0) is a sign of large dust particles; a high (up to 2) corresponds to small smoke particles. According to [34], typical values of the shaping factor are larger than 2.0 for fresh smoke particles and close to zero for Sahelian Saharan dust particles. The dust studies seem to yield shaping factors in the range of approximately 0.2, whereas particles produced from biomass burnings yielded shaping factors around 1.5 and higher. The formula is derived on the premise that the extinction of solar radiation by aerosols is a continuous function of wavelength, without selective bands or lines for scattering or absorption [35].

To quantify the water uptake at sub-saturated conditions, we define the hygroscopic growth factor (HGF) as the ratio of the radii of the mixture at a given RH (R_{RH}), to the original dry radius R_{dry}, which is at an RH=0%, [36-38]:

$$HGF = \frac{R_{RH}}{R_{dry}} \quad (6)$$

In this paper, HGF is calculated at 50, 70, 80, 90, 95, 98 and 99% RH. The HGF is subdivided into three different classes with respect hygroscopicity. One classification is based on diameter growth factor by [37, 39] as Barely Hygroscopic (BH; GF = 1.0–1.11), Less Hygroscopic (LH; GF = 1.11–1.33), More Hygroscopic (MH; GF = 1.33–1.85) .

The hygroscopic growth of aerosols also influences the particle size distribution and refractive indices and hence, several key optical properties of aerosols (e.g., scattering, extinction and absorption coefficients, single scattering albedo, asymmetry parameter, and aerosol optical depth) that are relevant to aerosol radiative forcing estimates [11-13].

The aerosol hygroscopic growth factor, f(RH, λ), that describes the ratio of aerosol light extinction between two different RH values at different wavelengths was calculated from the following [40]:

$$f(RH,\lambda) = \frac{\sigma_{ext}(RH_{high},\lambda)}{\sigma_{ext}(RH_{ref},\lambda)} = \left(\frac{100-RH_{ref}}{100-RH_{high}}\right)^{\gamma} \quad (7)$$

Where γ is referred to as the aerosol hygroscopicity factor. Hygroscopic properties of aerosol particles describe the interactions between particles and surrounding water vapor including the critical size needed to activate the growth of a particle into a cloud droplet by water vapor condensation in given conditions.

RESULTS AND DISCUSSIONS

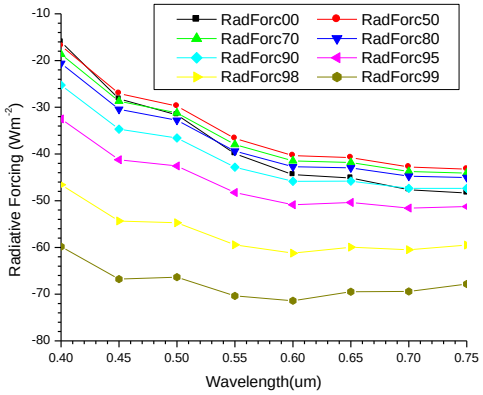

Figure 1: A graph of radiative forcing against wavelengths

Figure 1 shows that RF follows a relatively smooth decrease with wavelength for cases 0 to 80% RH, but as from 90% to 99% RH the graphs curved upward (the deliquescence point). It also shows that RF (cooling) increases with the increase in RH. The main reason is that, as a result of hygroscopic growth and/or coagulation, fine particles scatter more light than coarse particles. The relation of RF with RH is such that at the deliquescence point (90 to 99%) this growth with

higher humidities increases substantially, making this process strongly nonlinear with relative humidity [36,41].

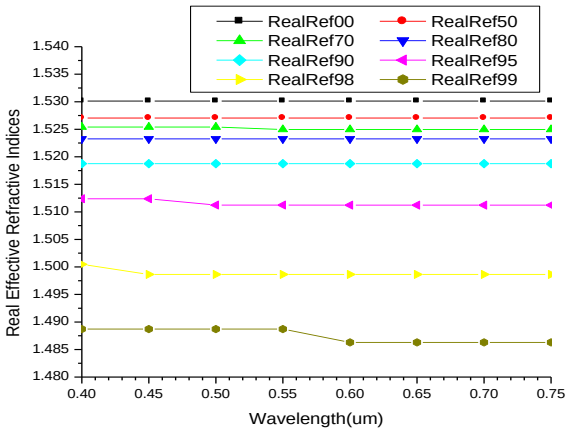

Figure 2: A plot of effective real refractive indices against wavelength

From figure 2 it can be seen that real effective refractive indices decreases with relative humidities. The relation of effective real refractive indices with RH is such that at the deliquescence point (90 to 99%) this decrease with higher humidities increases substantially, making this process strongly nonlinear with relative humidity [36, 41].

It is however constant in wavelength except at 95%, 98% and 99% where slight decreases can be seen, and these correspond to non-spherical particles (coarse particles) as pointed out by [42]. These variations may also be due to variations in the mixing state of different components of the aerosols due to changes in RH.

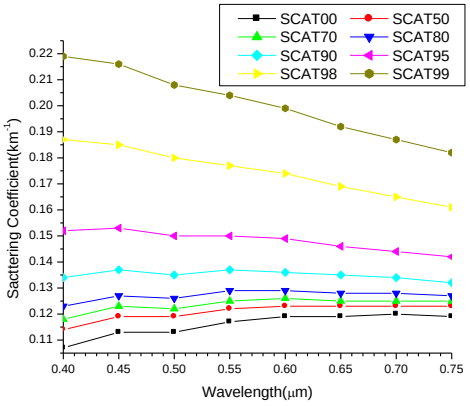

Figure 3: A graph of Scattering coefficients against wavelength.

Figure 3 shows that scattering increases with increasing RH. The relation of scattering coefficients with RH is such that at the deliquescence point (90 to 99%) this growth with higher humidities increases substantially, making this process strongly nonlinear with relative humidity [36,41,43,44]. The relation of scattering with wavelength is such that the relation between scattering coefficients is increasing with wavelength (positive slope), but as the RH increases the relation is decreasing until at 90% where it becomes straight but later started to be decreasing with the increase in wavelength up to 99%. This has happened because as a result of hygroscopic growth, smaller particles at shorter wavelength scatter more light than bigger (coarse) particles.

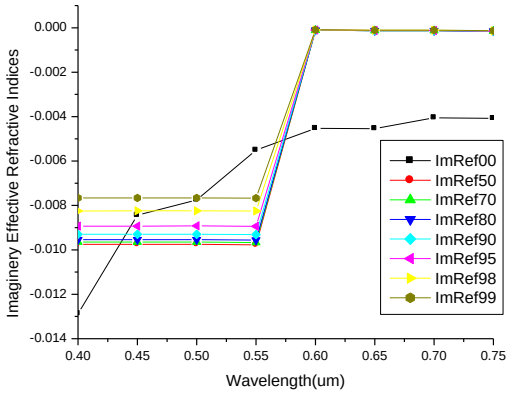

Figure 4: A plot of effective imaginary refractive indices against wavelengths

From figure 4, it can be seen that the relation between effective imaginary refractive indices with λ at RH=0 is that it increases smoothly upwards with the increase in wavelength, but as a result of hygroscopic growth it can be seen that it decreases in magnitude with RH from 0.4µm to 0.55µm but constant per wavelength. The nature of the graphs may be due to variations in the mixing state of different components of the aerosols due to the changes in RH. It is constant from 0.6µm to 0.75 µn both with respect to wavelength and RH.

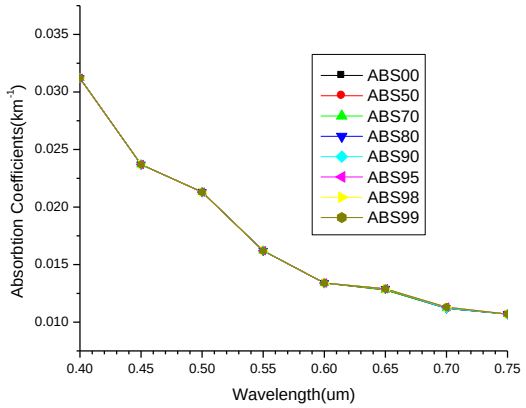

Figure 5: a graph of Absorption coefficients against wavelengths.

This shows that absorption coefficient is independent of hygroscopic growth and mode size distribution increase, but decreases smoothly with the increase in wavelengths. It can satisfy power law (equations 4 and 5).

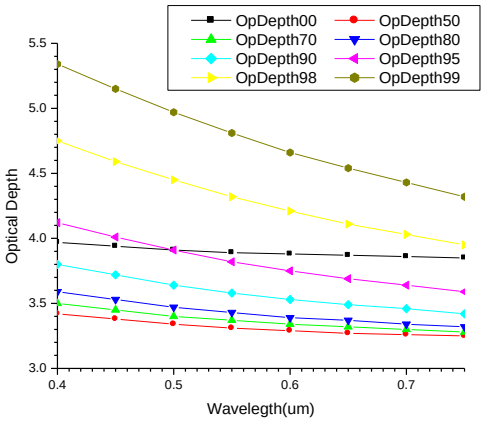

Figure 6: A graph of optical depth against wavelengths.

Figure 6 shows that the optical depth follows a relatively smooth decrease with wavelength for all cases and can be approximated with power law wavelength dependence (Optical Depth Angstrom Exponent or ODAE). This is in agreement with equations (4) and (5). From the figure it can be seen that there is a decrease in optical depth from 0% RH to 50%RH, which reflects decrease in mode size distributions as a result of hygroscopic growth. But as the RH increases there is an increase in optical depth which also results in the increase in mode size distributions.

It is evident from the figure that there is relatively strong wavelength dependence of optical depth at shorter wavelengths that gradually decreases towards longer wavelengths irrespective of the RH, attributing to the presence of fine particles. The presence of a higher concentration of the fine-mode particles which are selective scatters enhances the irradiance scattering in shorter wavelength only while the coarse-mode particles provide similar contributions to the AOD at both wavelengths [45]. It also shows that as a result of hygroscopic growth fine particles have more impact the coarse particles at smaller wavelengths. The relation of AOD with RH is such that at the deliquescence point (90 to 99%) this growth with higher humidities increases substantially, making this process strongly nonlinear with relative humidity [36,41]. It also

shows that power law (Junge power law) is well fitted in this spectral range as in [46]. A higher RH could obviously cause the particles' hygroscopic increase, which could result in greater extinction and a larger volume of fine particles.

Table 1: The results of the Angstron coefficients (from equation 5) at the respective relative humidities using regression analysis with SPSS15.

RH (%)	0	50	70	80	90	95	98	99
α	0.0466	0.0842	0.1038	0.12321	0.1653	0.2182	0.2934	0.3395
β	3.7937	3.1575	3.1743	3.1947	3.2530	3.3632	3.6283	3.9210
R^2	0.965	0.984	0.988	0.991	0.995	0.998	1.000	1.000

The observed variations in Ångström coefficients can be explained by changes in the effective radius of a mixture resulting from changes in RH: the larger the number of small aerosol particles, the smaller the effective radius and the larger the Ångström coefficient. From table 1 it can be seen that the value of α is less than 1, which reflect the dominance of large particles and the increase of α with the increase in RH happens as a result of hygroscopic growth. The high AOD is linked to a hygroscopic and/or coagulation growth from the fine aerosols. Furthermore, the fine mode aerosols have hydrate and coagulated characters that can make them to become large particles, causing the AOD to increase and/or to decrease. An increase in AOD with an increasing α as a result of change in RH, reflects the presence of fine particles in the aerosol size distribution. There is observational evidence that Ångström exponents decrease in value as particles grow hygroscopically [47].

Table 2: Values of Hygroscopic growth factor (HGF) equation(6), RH and volume mix ratio of WASO.

RH(%)	0	50	70	80	90	95	98	99
HGF	1.000	1.002	1.003	1.004	1.006	1.008	1.011	1.014
WASO(Vol. Mix %)	1.710	3.186	4.060	4.980	7.160	10.400	16.500	21.800

Table 2 is obtained using equation (6). It can be concluded that this mixture is barely hygroscopic (BH). This is not surprising because the percentage of WASO which is the part

responsible for water absorption component is very small. At the deliquescence point this growth with higher humidities increases substantially, making this process strongly nonlinear with relative humidity [36, 41].

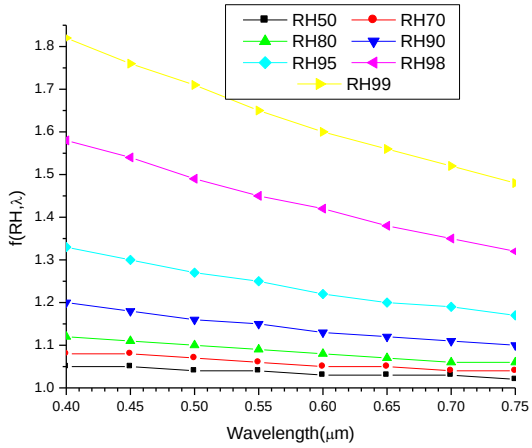

Figure 7: A graph of hygroscopic growth factor against wavelength (equation(7)).

Figure 7 shows a relatively smooth decrease with wavelength for all cases and can be approximated with power law wavelength dependence (equation 4). The relation of f(RH, λ) with RH is such that at the deliquescence point (90 to 99%) this growth with higher humidities increases substantially, making this process strongly nonlinear with relative humidity [36, 41]. This shows that power law (Junge power law) is well fitted in this spectral ranges as in [46].

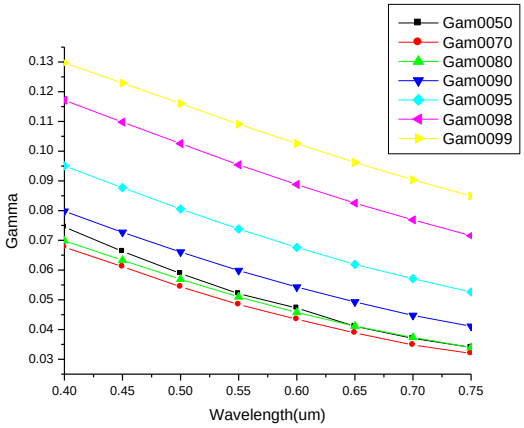

Figure 8: A graph of Gamma against wavelengths

Form figure 8, gamma which is described as the degree of hygroscopicity of aerosols with RH shows that the hygroscopicity is higher between 0and 50% RH than 0 to 70 and 0 to 80%. However the hygroscopicity started increasing with RH from 0 to 70, with a value of 0.06 to a maximum of 0.13 at 99% and at 0.4μm. The graph also shows that hygroscopicity decreases smoothly with the increase in wavelengths. This also satisfies power law. Also since γ is less than 1, this impies that the mixture is barely hygroscopic as can be seen in table 2.

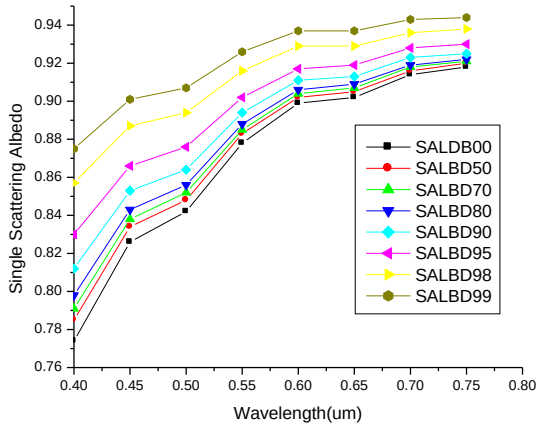

Figure 9: A graph of single scattering albedo against wavelengths.

Figure 9 shows that single scattering albedo increases smoothly with wavelength. This matches with the increase of scattering more than absorption. The relation of single scattering albedo with RH is such that at the deliquescence point (90 to 99%) this growth with higher humidities increases substantially, making this process strongly nonlinear with relative humidity [36, 41]. This also demonstrates the reason why Radiative cooling is increasing with RH. The inferred single scattering albedo lies in the range of 0.87 to 0.94, indicating significant aerosol scattering.

Many studies emphasize the importance of SSA , which represents the relative contribution s of aerosol scattering and absorption, in affecting the Earth-atmosphere radiation budget [48]. Aerosols with large SSA scatter the incoming solar radiation, cooling the atmosphere and surface. It is also discussed by [42, 49] that single scattering albedo increases with wavelength for dust particles. Such increase in SSA with wavelength is found to be common [50].

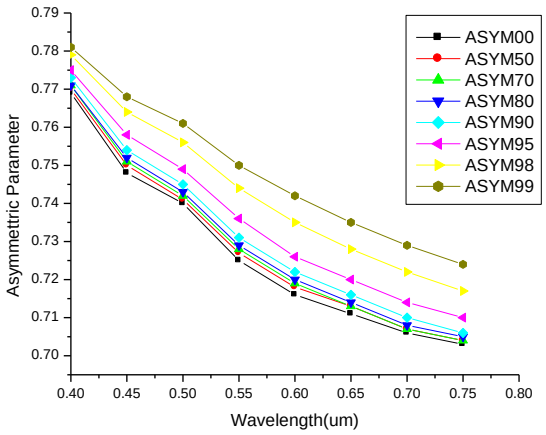

Figure 10: a graph of Asymmetry parameter against wavelengths.

This graph signifies the dominance of large particles as explained in figure 3. It also shows that the small particles scatter more light in the forward direction than backward. Its relation with RH shows that hygroscopic growth enhances scattering in the forward direction.

CONCLUSION

Analysis of the results showed that at 0% RH the radiative cooling increase steeply with wavelength, but at 50% the radiative cooling decreases which is in comparison with the decrease in optical depth and mode size distribution as shown in figure 6. As the RH increase the radiative cooling continued to increase which corresponds to increase in optical depth and mode size distributions. From the Angstrom coefficient, it increases with the increase in RH as a result of

hygroscopic growth and less than 1 throughout, which indicate that the particle distribution is dominated by coarse mode particles and it also satisfy power law type size distribution. The overall analyses led to the conclusion that the global mean short-wave radiative forcing is proportional to optical depth and mode size distributions and is negative due to the predominantly scattering nature of these aerosols in this solar spectral range as a result of the dominance of coarse particles.

REFERENCES

[1] Ackerman, P., and Toon O. B., (1981): Absorption of visible radiation in atmosphere containing mixtures of absorbing and non absorbing particles. Appl. Opt., 20, 3661-3668.

[2] Charlson, R. J., Schwartz S. E., Hales J. M., Cess D., Coakley J. A., Hansen J. E., (1992) Climate forcing by anthropogenic aerosols. Science, 255, 423-430.

[3] Stanhill, G. and Cohen S., (2001): Global dimming: a review of the evidence for a widespread and significant reduction in global radiation with discussion of its probable causes and possible agricultural consequences. Agricultural and Forest Meteorology, 107, 255-278.

[4] Che, H. Z., Shi G. Y., Zhang X. Y., Arimoto R., Zhao J. Q., Xu L., Wang B., and Chen Z. H., (2005) Analysis of 40 years of solar radiation data from China, 1961-2000. Geophys. Res. Lett., 32, L06803, doi: 10.1029/2004GL022322.

[5] Menon, S., Hansen J. E., Nazarenko L., and Luo Y. F. (2002): Climate effects of black carbon aerosols in China and India. Science, 297, 2249-2252.

[6] Andreae, M. O., (1995) Climatic effects of changing atmospheric aerosol levels, chap. 10, in World Survey of Climatology, vol. 16, Future Climates of the World, edited by A. Henderson-Sellers, pp. 347– 398, Elsevier Sci., New York,.

[7] Uematsu, M., Duce R. A., Prospero J. M., Chen L., Merrill J. T., and McDonald R. L., (1983): Transport of mineral aerosol from Asia over the North Pacific Ocean. J. Geophys. Res., 88, 5343-5352.

[8] Gong, S. L., Zhang X. Y., Zhao T. L., Mckendry I. G., Jaffe D. A., and Lu N. M., (2003) Characterization of soil dust aerosol in China and its transport/distribution during 2001 ACE-Asia, 2. Model Simulation and Validation. J. Geophys. Res., 108, 4262, doi: 10.1029/2002JD002633.

[9] Prospero, J. M., and Lamb P. J., (2003): African droughts and dust transport to the Caribbean: climate change implications, Science, 302, 1024- 1027.

[10] d'Almeida, G. A. , Koepk P. e , and Shettle E . P.(1991) Atmospheric Aerosols Global Climatology and Radiative Characteristics, A. Deepak, Hampton, Va.,.

[11] Penner, J.E., et al., (1994). Quantifying and minimizing uncertainty of climate forcing by anthropogenic aerosols. Bulletin of the American Meteorological Society 75, 375–400.

[12] IPCC (2001): Climate Change 2001: The Scientific Basis. Houghton et al., Eds., Cambridge University Press, New York. 896 pp.

[13] Carrico, C.M., Kus, P., Rood, M.J., Quinn, P.K., Bates, T.S., (2003). Mixtures of pollution, dust, sea salt, and volcanic aerosol during ACE-Asia: radiative properties as a function of relative humidity. Journal of Geophysical Research 108 (D23), 8650.

[14] Kotchenruther, R. A., Hobbs P. V. and Hegg D. A.(1999) Humidification factors for atmospheric aerosols off the mid-Atlantic coast of the United States, J. Geophys. Res., 104, 2239 – 2251,.

[15] Im, J. S., Saxena V. K., and Wenny B. N.(2001) An assessment of hygroscopic growth factors for aerosols in the surface boundary layer for computing direct radiative forcing, J. Geophys. Res., 106, 20,213 – 20,224.

[16] Hegg, D.A., Covert, D.S., Crahan, K., 2002. The dependence of aerosol light scattering on RH over the Pacific Ocean. Geophysical Research Letters 29 (8), 1219.

[17] Magi, B.I., Hobbs, P.V., (2003). Effects of humidity on aerosols in Southern Africa during the biomass burning season. Journal of Geophysical Research 108 (D13), 8495.

[18] MaXling, A., Wiedensohler, A., Busch, B., NeusuX, C., Quinn, P., Bates, T., Covert, D., (2003). Hygroscopic properties of different aerosol types over the Atlantic and Indian Oceans. Atmospheric Chemistry and Physics 3, 1377–1397.

[19] Maria, S.F., Russell, L.M., Gilles, M.K., Myneni, S.C.B., (2004). Organic aerosol growth mechanisms and their climate-forcing implications. Science 306, 1921–1924.

[20] White, W.H., Roberts, P.T., (1977). On the nature and origins of visibility-reducing aerosols in the Los Angeles air basin. Atmospheric Environment 11, 803–812.

[21] Tang, I.N., Wong, W.T., Munkelwitz, H.R., (1981). The relative importance of atmospheric sulfates and nitrates in visibility reduction. Atmospheric Environment 12, 2463–2471.

[22] Malm, W.C., Day, D.E., Kreidenweis, S.M., Collett, J.L., Lee, T., (2003). Humidity-dependent optical properties of fine particles during the big bend regional aerosol and visibility observational study. Journal of Geophysical Research 108 (D9), 4279.

[23] Hess M., Koepke P., and Schult I (May 1998), Optical Properties of Aerosols and Clouds: The Software Package OPAC, Bulletin of the A merican Met. Soc. **79**, 5, p831-844.

[24] Chylek P. and Wong J. (1995), Effect of Absorbing aerosols of global radiation budget, Geophysical Research Letters, 22, 8, p929-931

[25] Penner, J. E. Dickinson R.E. and O'Neil C. A. (1992) Effects of aerosols form biomass on the global radiation budget, Science, 256, 1432-1434.

[26] Segan, C. and Pollack J.(1967) Anisotropic nonconservative scattering and the clouds of Venus, J. Geophys. Res., 72, 469-477.

[27] Aspens D. E. (1982), Local-field effect and effective medium theory: A microscopic perspective Am. J. Phys. 50, 704-709.

[28] Lorentz, H. A. (1880). Ueber die Beziehung zwischen der Fortpflanzungsgeschwindigkeit des Lichtes und der Korperdichte. Ann. P hys. Chem. 9, 641–665.

[29] Lorenz, L. (1880). Ueber die Refractionconstante. A nn. P hys. Chem. 11, 70–103.

[30] Holben, B.N., D. Tanre, A. Smirnov, et al., An emerging ground-based aerosol climatology: Aerosol optical depth from AERONET. J. Geophys. Res., 106, 12,067-12,097, 2001.

[31] Liou K. N. (2002) An Introduction to Atmospheric Radiation, 2nd ed. Academic, San Diego, Calif.,.

[32] O'Neill N. T., and Royer A. (1993) Extraction of binomial aerosol-size distribution radii from spectral and angular slope (Angstrom) coefficients, Appl. Opt. 32, 1642-1645.

[33] Dubovik, O., et. al., (2000): Accuracy assessments of aerosol optical properties retrieved from Aerosol Robotic Network (AERONET) Sun and sky radiance measurments, JGR, 105, 9791 - 9806.

[34] Eck, T. F., et al. (2005), Columnar aerosol optical properties at AERONET sites i n cen tr al easte rn Asia a nd aer osol tr anspor t t o t he tropic al mid -Pacific, J. Geophys. Res. , 110 , D06202, doi:10.1029/2004JD005274

[36] Tang, I. N. (1996) Chemical and size effects of hygroscopic aerosols on light scattering coeffcients. J. Geophys . Res., 101, 19245 – 19250

[37] Swietlicki, E.,et. al. (2008) Hygroscopic properties of submicrometer atmospheric aerosol particles mea-sured with H TDMA instruments in various environments – A review, Tellus B, 60, 432–469,.

[38] Randles , C. A. , Russell L. M. and. Ramaswamy V. (2004) Hygroscopic and optical properties of organic sea salt aerosol and consequences for climate forcing, Geophys. Res. Let., 31, L16108, doi:10.1029/2004GL020628.

[39] Liu P. F., Zhao C. S., Gobel T., Hallbauer E., Nowak A., Ran L., Xu W. Y., Deng Z. Z., Ma N., Mildenberger K., Henning S., Stratmann F., and Wiedensohler A. (2011) Hygroscopic proper ties of aerosol par ticles at high relative humidity and their diurnal variations in the Nor th China Plain, Atmos. Chem. Phys. Discuss., 11, 2991–3040

[40] Doherty, S. J., Quinn P. K., Jefferson A., Carrico C. M., Anderson T. L., and Hegg D. (2005), A comparison and summary of aerosol optical properties as observed in situ from aircraft, ship, and land during ACE-Asia, J. Geophys. Res., 11 0 , D04201, doi:10.1029/2004JD004964.

[41] Fitzgerald , J. W. (1975) Approximation formulas for the equilibrium size of an aerosol particle as a function of its dry size and composition and ambient relative humidity. J. Appl . Meteorol. , 14, 1044 –1049.

[41] Hansen, J., M. Sato, A. Lacis, R. Ruedy, I. Tegen, and E. Matthews (1998), Climate forcings in the Industrial era, Proc. Natl. Acad. Sci. U. S. A., 95, 12,753 – 12,758, doi:10.1073/pnas.95.22.12753.

[42] Dubovik, O., et. al., (2002): Variability of Absorption and Optical Properties of Key Aerosol Types Observed in Worldwide Locations, J. Atmos. Sci., 59, 590 – 608.

[43] Anderson, T. L. and Ogren, J. A.:(1998) Determining aerosol radiative properties using the TSI 3563 integrating nephelometer, Aerosol. Sci. Tech., 29, 57–69,.

[44] Xu, J., Bergin, M. H., Yu, X., Liu, G., Zhao, J., Carrico, C. M., and Baumann, K.:(2002) Measurement of aerosol chemical, physical and radiative properties in the Yangtze delta region of China, Atmos. Environ., 36, 161–173.

[45] Schuster, G.L., Dubovik, O. and Holben, B.N. (2006). Angstrom Exponent and Bimodla Aerosol Size Distributions. J. Geophy. Res. 111: 7207.

[46] Eck, T.F., B.N.Holben, J.S.Reid, O.Dubovik, A.Smirnov, N.T.O'Neill, I.Slutsker, and S.Kinne, (1999), The wavelength dependence of the optical depth of biomass burning, urban and desert dust aerosols, J.Geoph.Res., 104, 31,333-31,350,.

[47] Carrico, C.M., Rood, M.J., Ogren, J.A.,(1998) Aerosol light scattering properties at Cape Grim, Tasmania, during the First Aerosol Characterization Experiment (ACE 1), J. Geophys. Res ., 103, 16565-16574.

[49] Bergstrom, R. W., Russell, P. B., and Hignett, P. B(2002) The wavelength dependence of black carbon particles: predictions and results from the TARFOX experiment and implications for 20 the aerosol single scattering albedo, J. Atmos. Sci., 59, 567–577.

[50] Kubilay, N., Cokacar, T., Oguz, T., (2003). Optical properties of mineral dust outbreaks over the northeastern Mediterranean. Journal of Geophysical Research Atmospheres 108 (D21), 4666.